Research Article

INTERNATIONAL JOURNAL OF ADVANCED ROBOTIC SYSTEMS

International Journal of Advanced Robotic Systems
November-December 2016: 1–10

DOI: 10.1177/1729881416662792
arx.sagepub.com
SAGE

Electromechanical coupling vibration characteristics of an AC servomotor-driven translational flexible manipulator

Jin-yong Ju[1], Wei Li[2], Xue-Feng Yang[1], Yu-Qiao Wang[1], and Yu-Fei Liu[1]

Abstract

The nonstationary transition status of the motor start-up phase creates great threat against the stable operation of the flexible manipulator system. This article investigates the electromechanical coupling dynamics and vibration response characteristics for a flexible manipulator of an alternating current servomotor-driven linear positioning platform with considering the start-up dynamic characteristics of the motor. Based on the constructed global electromechanical coupling effect and the Lagrange–Maxwell equations, the dynamic model of the whole system is established. The electromechanical coupling vibration mechanism of the flexible manipulator is obtained by analyzing the multiphysical process and multi-parameter coupling phenomenon of the whole system. The result demonstrates that the nonstationary transition status of the motor initialization phase is mainly manifested during the disturbance of the three-phase stator current. As the speed of the linear positioning platform increases, the current disturbance, arousing the change of the servo driving force of the linear positioning platform, has dominant frequency shift and frequency amplitude decrease. Then, the vibration response of the flexible manipulator is markedly affected and the variation of the high-order modes vibration response is more obvious. The analysis result is significant for improving the dynamic performance of the motor-driven flexible robot manipulator system.

Keywords

Flexible manipulator, linear positioning platform, electromechanical coupling dynamics, Lagrange–Maxwell equations, vibration characteristics

Date received: 23 February 2016; accepted: 14 June 2016

Topic: Robot Manipulation and Control
Topic Editor: Andrey V Savkin

Introduction

As the modern robot technology is developing to lower energy consumption, higher speed, and higher precision, there has been increasing attention on the flexible manipulator.[1–4] Compared with the rigid manipulator, the flexible manipulator has many advantages such as lower energy consumption, higher load weight ratio, and higher speed. Thus, it has been widely adopted in precision assembly,[5] space equipment,[6] and modern manufacturing processes.[7,8] However, owing to the feeble rigidity and heavy deflection, the flexible manipulator exhibits a long elastic vibration in rapid positioning, which seriously impacts the positioning speed and accurate tracking ability of the whole system. Therefore, the vibration mechanism and control strategy of the flexible manipulator have always been a quite focused issue.[9–11]

[1] School of Mechatronic Engineering, China University of Mining and Technology, Xuzhou, China
[2] China University of Mining and Technology, Xuzhou, China

Corresponding author:
Wei Li, China University of Mining and Technology, University Road No. 1, Xuzhou 221116, China.
Email: liweicumt@163.com

Before a reasonable and effective active vibration control algorithm is designed, the vibration mechanism of the flexible manipulator system should be obtained first. Most of the existing investigations focus on the effect of the parameters of the flexible manipulator itself on its dynamic characteristics. Coleman and McSweeney derived the eigenspectrum and eigenfunctions and investigated the behavior of the spectrum of a flexible manipulator while the base movement was described as zero-disturbance.[12] In the study by Qiu,[13] the vibration control of a Cartesian flexible manipulator was studied by ignoring the interference of the base. Abe[14] suppressed the vibration of a flexible Cartesian robot manipulator through planning the trajectory of its base while the exact mathematical model was aim to the flexible manipulator itself. However, the flexible manipulator system is mainly made up of the base driving devices and the upper flexible actuators.[15–17] Due to the fluctuation of motor electromagnetic parameters and the structural inertia, it is very difficult to move with strict uniform velocity or constant axial force for the driving system, especially when the motion state changes.

With the base's ripple components of the transmission speed or the axial force considered, the lateral movement of the flexible manipulator is likely to present complicated dynamical characteristics, and large amplitude vibration appears, which is caused by the parametric excitation vibration.[18,19] Therefore, it is very important to consider the effect of the base's dynamic characteristics on the vibration characteristics of the flexible manipulator system. In the study by Pratiher and Dwivedy,[20] the influence of base excitation on the steady-state response of the flexible manipulator was studied by describing the interference of the base as harmonic excitation. Dwivedy and Kar investigated the nonlinear dynamic characteristics of a parametrically excited cantilever beam, the base of which was under harmonic excitation.[21] Liu studied the vibration response of a flexible manipulator which was driven by a moving base and confirmed that the rigid base, with its motion disturbances, had a significant influence on the vibration response.[22] Moreover, in order to satisfy the system's requirements of high accuracy, high-speed performance, and strong adaptability, the alternating current (AC) servomotors are often adopted for the base driving devices of the flexible robot manipulator. Li studied the nonlinear dynamic characteristics of a linkage mechanism system, which was driven by a three-phase AC motor and indicated that the electromagnetic parameters had significant effects on the linkage mechanism system.[23] In another study, with the inconstant speed of the direct current (DC) motor considered, the dynamic response of a motor–gear mechanism system was analyzed. [24] For the motor-driven flexible manipulator system, the dynamic performance of the base is to a great extent determined by the output characteristic of the motor. However, the motor's output is not ideally constant, but fluctuation exists, especially at the start-up stage. The motion fluctuation will further affect the vibration characteristics of the flexible robot manipulator. In addition, there are few reports on the special vibration characteristics of the flexible robot manipulator under the disturbance stimuli of special driving equipment. Besides, the relationship between the disturbance stimuli and the movement characteristics should be further studied. Therefore, in order to accurately analyze the vibration characteristics of the flexible manipulator and apply effective vibration control, the motion fluctuations of the motor should be taken into consideration.

Fortunately, based on the analysis dynamics theory of electromechanical system and Lagrange–Maxwell equations, the global coupling dynamic model of the AC servomotor-driven flexible manipulator is constructed in this article. Then, the electromechanical coupling between the AC servomotor and the flexible manipulator is intensively studied to demonstrate the global electromechanical coupling relationship diagram of the flexible manipulator of an AC servomotor-driven linear positioning platform. Furthermore, under the direct coupling of electromagnetic torque, the electromechanical coupling vibration characteristics of the flexible manipulator are investigated.

The structure of this article is organized as follows: The section "Electromechanical coupling dynamic modeling" describes the electromechanical coupling dynamic model of the flexible manipulator of an AC servomotor-driven linear positioning platform. In the section "Decoupling analysis of the electromechanical coupling vibration", the decoupling analysis for the electromechanical coupling dynamic model is exhibited and the motor parameters, which have main influence on the elastic vibrations of the flexible manipulator, are provided. Then, a simulative example is introduced in the section 'Simulation examples' and the specific relationship between the motor parameters and the vibration response of the flexible manipulator is presented. The section 'Conclusions' concludes this study.

Electromechanical coupling dynamic modeling

The flexible manipulator system of a linear positioning platform, driven by an AC servomotor, is a complex electromechanical system that includes motor subsystem, transmission subsystem, control subsystem, and perform subsystem. For its dynamics characteristics, the flexible manipulator is affected not only by its own structure parameters but also by other coupling subsystems. Therefore, the global electromechanical coupling relationship diagram, which is shown in Figure 1, should be revealed to analyze the specific coupling form of the AC servomotor-driven translational flexible manipulator.

Owing to the fact that the motor subsystem is the direct driving source of the whole system, the direct coupling of electromagnetic torque, which is the basic form of the electromechanical coupling, is analyzed in this article. A schematic diagram of an AC servomotor-driven translational flexible manipulator is shown in Figure 2. The slider, which is rigidly connected to the flexible manipulator by bolts, is driven by an AC servomotor and a ball screw. During the modeling process, assumptions are made as follows: (1) the

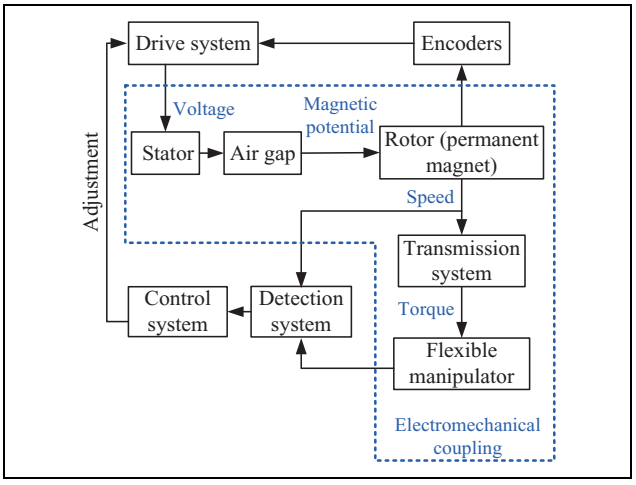

Figure 1. Global electromechanical coupling relationship diagram of the AC servomotor-driven translational flexible manipulator. AC: alternating current.

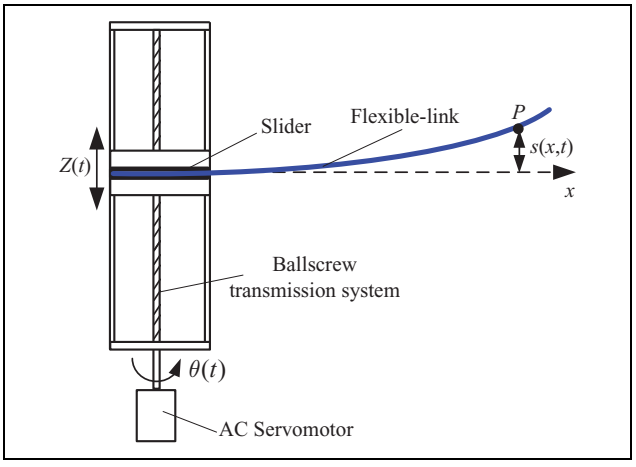

Figure 2. Schematic diagram of an AC servomotor-driven translational flexible manipulator. AC: alternating current.

influences of temperature and frequency on the motor parameters are neglected; (2) the motor air gap is uniform; (3) the self-inductance and mutual-inductance among the motor three-phase windings are assumed as constants; (4) the flexible manipulator is simplified as an Euler–Bernoulli beam by neglecting the impact of shear and axial deformation; and (5) the influence of gravity is ignored.

The electromechanical coupling dynamic models of the AC servomotor-driven translational flexible manipulator are constructed by Lagrange–Maxwell equations which can be expressed as

$$L = T_{\text{mech}} + W_{\text{m}} - U \tag{1}$$

where T_{mech} is the kinetic energy of the AC servomotor-driven translational flexible manipulator system, U is the elastic potential energy of the flexible manipulator, and W_{m} denotes the magnetic field energy of the AC servomotor.

Assuming that the AC servomotor-driven translational flexible manipulator system has N degrees of freedom, its Lagrange–Maxwell equations can be given as[25]

$$\frac{\mathrm{d}}{\mathrm{d}t}\left(\frac{\partial L}{\partial \dot{q}_m}\right) - \frac{\partial L}{\partial q_m} + \frac{\partial F_h}{\partial \dot{q}_m} = Q_m, \quad m = 1, 2, \ldots, N \tag{2}$$

where Q_m denotes generalized force that corresponds to generalized coordinates q_m and F_h is the dissipation function of the whole system.

1. The whole kinetic energy of the AC servomotor-driven translational flexible manipulator system includes four parts: the motor shaft, the screw, the solider, and the flexible manipulator. Besides, the kinetic energy of the screw and the solider can be equaled to the motor shaft and the equivalent rotary inertia of the motor shaft can be written as

$$J_m = J_d + \left[\frac{MD^2}{8} + \left(\frac{p}{2\pi}\right)^2 W\right] \tag{3}$$

where J_d is the rotary inertia of the motor shaft, W is the quality of the solider, and M, D, and P are the quality, diameter, and lead of the screw, respectively.

As a consequence, the kinetic energy of the AC servomotor-driven translational flexible manipulator system can be represented as:

$$T_{\text{mech}} = \frac{1}{2}J_m\dot{\theta}^2 + \frac{1}{2}\int_0^L \rho A\left[\frac{p}{2\pi}\dot{\theta} + \dot{s}(x,t)\right]^2 dx \tag{4}$$

where θ signifies the motor angle, $s(x, t)$ is the transverse vibration displacement of the flexible manipulator, and L, ρ, and A are the length, density, and cross-sectional area of the flexible manipulator, respectively.

2. The AC servomotor is chosen as a permanent magnet synchronous AC servomotor (PMSM) due to its good low-speed characteristics and excellent speed control performance. Then, the magnetic energy, caused by the stator current itself as well as the interaction of the stator current and the flux linkage of the permanent magnet rotor, constitutes the whole magnetic field energy of the motor and can be expressed as

$$\begin{aligned} W_m = {} & \frac{1}{2}\sum_j\sum_n L_{jn}i_j i_n + i_A\psi_f\cos\theta + i_B\psi_f\cos\left(\theta - \frac{2}{3}\pi\right) \\ & + i_C\psi_f\cos\left(\theta + \frac{2}{3}\pi\right) = \frac{1}{2}L_A i_A^2 + \frac{1}{2}L_B i_B^2 \\ & + \frac{1}{2}L_C i_C^2 + Hi_A i_B + Hi_A i_C + Hi_B i_C + i_A\psi_f\cos\theta \\ & + i_B\psi_f\cos\left(\theta - \frac{2}{3}\pi\right) + i_C\psi_f\cos\left(\theta + \frac{2}{3}\pi\right) \end{aligned} \tag{5}$$

where i_A, i_B, and i_C indicate the current of the three-phase stator, L_A, L_B, and L_C are the self-inductance of the three-phase windings, H is the mutual-inductance, and ψ_f is the flux linkage of the permanent magnet rotor.

3. The elastic potential energy of the flexible manipulator can be represented as

$$U = \frac{1}{2}\int_0^L EI\left[\frac{\partial^2 s(x,t)}{\partial x^2}\right]^2 \mathrm{d}x \tag{6}$$

where E and I are the elastic modulus and moment of inertia of the flexible manipulator, respectively.

4. The dissipation function of the whole system includes the heat dissipation of the motor resistance and the rotation resistance dissipation of the motor rotor which is given as

$$F_h = \frac{1}{2}R_A i_A^2 + \frac{1}{2}R_B i_B^2 + \frac{1}{2}R_C i_C^2 + \frac{1}{2}R_n\dot{\theta}^2 \tag{7}$$

where R_A, R_B, and R_C are the resistance of the motor three-phase windings and R_n is the rotation resistance coefficient of the motor rotor.

5. For the electromagnetic system, the nonconservative force is the input voltages of the three-phase stator. Additionally, for the mechanical system, the nonconservative force is the frictional resistance between the slider and the guide rail and can be expressed as

$$Q_5 = -\upsilon_c(W + M + \rho AL) \tag{8}$$

where υ_c is the friction coefficient between the slider and the guide rail.

By substituting equations (4) to (6) into equation (1), the Lagrange–Maxwell operator can be written as

$$\begin{aligned} L = {} & \frac{1}{2}J\dot{\theta}^2 + \frac{1}{2}\int_0^L \rho A\left[\frac{p}{2\pi}\dot{\theta} + \dot{s}(x,t)\right]^2 \mathrm{d}x \\ & + \frac{1}{2}\sum_j\sum_n L_{jn} i_j i_n + i_A\psi_f\cos\theta + i_B\psi_f\cos\left(\theta - \frac{2}{3}\pi\right) \\ & + i_C\psi_f\cos\left(\theta + \frac{2}{3}\pi\right) - \frac{1}{2}\int_0^L EI\left[\frac{\partial^2 s(x,t)}{\partial x^2}\right]^2 \mathrm{d}x \end{aligned} \tag{9}$$

The generalized coordinates include: the three-phase stator charge (e_A, e_B, e_C) of the PMSM, the motor angle (θ), and the transverse vibration displacement of the flexible manipulator ($s(x,t)$). For A phase of the stator windings ($q_1 = e_A$), substitution of equation (9) into equation (2) leads to

$$\begin{aligned} & \frac{\mathrm{d}}{\mathrm{d}t}\left(\frac{\partial L}{\partial \dot{q}_1}\right) - \frac{\partial L}{\partial q_1} + \frac{\partial F_h}{\partial \dot{q}_1} = \frac{\mathrm{d}}{\mathrm{d}t}\left(\frac{\partial L}{\partial i_A}\right) + \frac{\partial F_h}{\partial i_A} \\ & = L_A\frac{\mathrm{d}i_A}{\mathrm{d}t} + H\frac{\mathrm{d}i_B}{\mathrm{d}t} + H\frac{\mathrm{d}i_C}{d\,\mathrm{t}} - \psi_f\dot{\theta}\sin\theta + R_A i_A \end{aligned} \tag{10}$$

Thus, the voltage equation of A stator winding can be written as

$$L_A\frac{\mathrm{d}i_A}{\mathrm{d}t} + H\frac{\mathrm{d}i_B}{\mathrm{d}t} + H\frac{\mathrm{d}i_C}{\mathrm{d}t} - \psi_f\dot{\theta}\sin\theta + R_A i_A = u_A \tag{11}$$

Similarly, the voltage equations of B and C stator winding are deduced to

$$L_B\frac{\mathrm{d}i_B}{\mathrm{d}t} + H\frac{\mathrm{d}i_A}{\mathrm{d}t} + H\frac{\mathrm{d}i_C}{\mathrm{d}t} - \psi_f\dot{\theta}\sin\left(\theta - \frac{2}{3}\pi\right) + R_B i_B = u_B \tag{12}$$

$$L_C\frac{\mathrm{d}i_C}{\mathrm{d}t} + H\frac{\mathrm{d}i_A}{\mathrm{d}t} + H\frac{\mathrm{d}i_B}{\mathrm{d}t} - \psi_f\dot{\theta}\sin\left(\theta + \frac{2}{3}\pi\right) + R_C i_C = u_C \tag{13}$$

For the mechanical system, when the generalized coordinate is the motor angle ($q_4 = \theta$), the followings are available.

$$\begin{cases} \dfrac{\partial L}{\partial q_4} = \dfrac{\partial L}{\partial \theta} = -i_A\psi_f\sin\theta - i_B\psi_f\sin\left(\theta - \dfrac{2}{3}\pi\right) \\ \qquad\qquad -i_C\psi_f\sin\left(\theta + \dfrac{2}{3}\pi\right) \\ \dfrac{\mathrm{d}}{\mathrm{d}t}\left(\dfrac{\partial L}{\partial \dot{q}_4}\right) = \dfrac{\mathrm{d}}{\mathrm{d}t}\left(\dfrac{\partial L}{\partial \dot{\theta}}\right) = J\ddot{\theta} + \dfrac{p}{2\pi}\left[\rho AL\ddot{\theta} + \displaystyle\int_0^L \rho A\ddot{s}(x,t)\,\mathrm{d}x\right] \\ \dfrac{\partial F_h}{\partial \dot{q}_4} = R_n\dot{\theta} \end{cases} \tag{14}$$

Then, the torque equation of the mechanical system can be represented as

$$\begin{aligned} & J\ddot{\theta} + \frac{p}{2\pi}\left[\rho AL\ddot{\theta} + \int_0^L \rho A\ddot{s}(x,t)\,\mathrm{d}x\right] + R_n\dot{\theta} + i_A\psi_f\sin\theta \\ & \quad + i_B\psi_f\sin\left(\theta - \frac{2}{3}\pi\right) + i_C\psi_f\sin\left(\theta + \frac{2}{3}\pi\right) \\ & = -\upsilon_c(W + M + \rho AL) \end{aligned} \tag{15}$$

When the generalized coordinate is the transverse vibration displacement of the flexible manipulator ($q_5 = s(x,t)$), the derivation process of the vibration equation for the flexible manipulator can be given as

$$\begin{aligned} & \frac{\mathrm{d}}{\mathrm{d}t}\left(\frac{\partial L}{\partial \dot{q}_5}\right) - \frac{\partial L}{\partial q_5} + \frac{\partial F_h}{\partial \dot{q}_5} = \frac{\mathrm{d}}{\mathrm{d}t}\left(\frac{\partial L}{\partial \dot{s}(x,t)}\right) + \frac{\partial F_h}{\partial \dot{s}(x,t)} \\ & \quad = \int_0^L \rho A\frac{p}{2\pi}\ddot{\theta}\,\mathrm{d}x + \int_0^L \rho A\ddot{s}(x,t)\,\mathrm{d}x + \int_0^L EI\frac{\partial^4 s(x,t)}{\partial x^4}\,\mathrm{d}x \end{aligned} \tag{16}$$

Then, the vibration equation can be expressed as

$$\rho A\frac{p}{2\pi}\ddot{\theta} + \rho A\ddot{s}(x,t) + EI\frac{\partial^4 s(x,t)}{\partial x^4} = 0 \tag{17}$$

Combining equations (11) to (13), (15), and (17), the electromechanical coupling dynamic models of the flexible manipulator of an AC servomotor-driven linear positioning platform are attainable and can be expressed as

$$\begin{cases} L_A\dfrac{\mathrm{d}i_A}{\mathrm{d}t}+H\dfrac{\mathrm{d}i_B}{\mathrm{d}t}+H\dfrac{\mathrm{d}i_C}{\mathrm{d}t}-\psi_f\dot{\theta}\sin\theta+R_Ai_A=u_A \\ L_B\dfrac{\mathrm{d}i_B}{\mathrm{d}t}+H\dfrac{\mathrm{d}i_A}{\mathrm{d}t}+H\dfrac{\mathrm{d}i_C}{\mathrm{d}t}-\psi_f\dot{\theta}\sin\left(\theta-\dfrac{2}{3}\pi\right)+R_Bi_B=u_B \\ L_C\dfrac{\mathrm{d}i_C}{\mathrm{d}t}+H\dfrac{\mathrm{d}i_A}{\mathrm{d}t}+H\dfrac{\mathrm{d}i_B}{\mathrm{d}t}-\psi_f\dot{\theta}\sin\left(\theta+\dfrac{2}{3}\pi\right)+R_Ci_C=u_C \\ J\ddot{\theta}+\dfrac{p}{2\pi}\left[\rho AL\ddot{\theta}+\displaystyle\int_0^L\rho A\ddot{s}(x,t)\,\mathrm{d}x\right]+i_A\psi_f\sin\theta \\ +i_B\psi_f\sin\left(\theta-\dfrac{2}{3}\pi\right)+i_C\psi_f\sin\left(\theta+\dfrac{2}{3}\pi\right)+R_n\dot{\theta} \\ =-\upsilon_c(W+M+\rho AL) \\ \rho A\frac{p}{2\pi}\ddot{\theta}+\rho A\ddot{s}(x,t)+EI\frac{\partial^4s(x,t)}{\partial x^4}=0 \end{cases} \tag{18}$$

From equation (18), it is obvious that the electromechanical coupling performance between the driving current of the PMSM and the transverse vibration displacement of the flexible manipulator is strong.

Decoupling analysis of the electromechanical coupling vibration

Using the assumed mode method, the transverse vibration of the flexible manipulator is given by

$$s(x,t)=\sum_{k=1}^{k\to\infty}\phi_k(x)q_k(t) \tag{19}$$

where $\phi_k(x)$ is the k-th modal shape and $q_k(t)$ is the corresponding modal coordinates.

Substituting equation (19) into equations (15) and (17) leads to:

$$\begin{aligned}&\left(J+\frac{p}{2\pi}\rho AL\right)\ddot{\theta}+\sum_{k=0}^{\infty}\int_0^L\rho A\phi_k(x)\,\mathrm{d}x\ddot{q}_k(t)+R_n\dot{\theta}\\&\quad+\upsilon_c(W+M+\rho AL)=-i_A\psi_f\sin\theta\\&\quad-i_B\psi_f\sin\left(\theta-\frac{2}{3}\pi\right)-i_C\psi_f\sin\left(\theta+\frac{2}{3}\pi\right)\end{aligned} \tag{20}$$

$$\rho A\frac{p}{2\pi}\ddot{\theta}+\sum_{k=0}^{\infty}\rho A\phi_k(x)\ddot{q}_k(t)+EI\frac{\partial^4s(x,t)}{\partial x^4}=0 \tag{21}$$

According to the structural mechanics, equation (21) can be translated into

$$\rho A\frac{p}{2\pi}\ddot{\theta}+\sum_{k=0}^{\infty}\rho A\phi_k(x)\ddot{q}_k(t)+\sum_{i=0}^{\infty}\rho A\lambda_k^2\phi_k(x)q_k(t)=0 \tag{22}$$

where λ_k is the k-th natural frequency of the flexible manipulator.

In accordance with the orthogonality of the modal shapes, equation (22) can be further simplified as

$$\frac{p}{2\pi}\int_0^L\rho A\phi_k(x)\,\mathrm{d}x\ddot{\theta}+\rho A\ddot{q}_k(t)+\rho A{\lambda_k}^2q_k(t)=0 \tag{23}$$

Because only the first several order modes play a leading role in the vibrations of the flexible manipulator, only the first four order modes are taken into consideration. By defining $m_k=\displaystyle\int_0^L\rho A\phi_k(x)\,\mathrm{d}x$, equations (20) and (23) can be reduced to

$$\begin{aligned}&\left(J+\frac{p}{2\pi}\rho AL\right)\ddot{\theta}+\sum_{k=1}^{4}m_k\ddot{q}_k(t)+R_n\dot{\theta}+\upsilon_c(W+M+\rho AL)\\&\quad=-i_A\psi_f\sin\theta-i_B\psi_f\sin\left(\theta-\frac{2}{3}\pi\right)-i_C\psi_f\sin\left(\theta+\frac{2}{3}\pi\right)\end{aligned} \tag{24}$$

$$\left\{\frac{p}{2\pi}m_k\ddot{\theta}+\rho A\ddot{q}_k(t)+\rho A{\lambda_k}^2q_k(t)=0\right\}_{k=1,2,3,4} \tag{25}$$

According to equation (18), the PMSM models are of strong coupling and nonlinearity, which is the reason why the traditional control strategies have heavy difficulty and challenges in the realization of high-performance speed regulation for the PMSM. Therefore, under the condition of the production of same magnetomotive force, the coordinate transformation is often adopted to equal three-phase AC windings to two-phase DC windings. Then, the PMSM, whose models are simplified and some variables are decoupled, can obtain good static and dynamic properties as DC adjustable speed system.

The Clarke transformation and Park transformation are essential for the three-phase AC windings transforming to two-phase DC windings. The constant power transformation is adopted and the synthetic transformation matrix can be derived as

$$T_p=\frac{\sqrt{6}}{3}\begin{bmatrix}\cos\theta & \cos\left(\theta-\dfrac{2\pi}{3}\right) & \cos\left(\theta+\dfrac{2\pi}{3}\right)\\ -\sin\theta & -\sin\left(\theta-\dfrac{2\pi}{3}\right) & -\sin\left(\theta+\dfrac{2\pi}{3}\right)\\ \dfrac{\sqrt{2}}{2} & \dfrac{\sqrt{2}}{2} & \dfrac{\sqrt{2}}{2}\end{bmatrix} \tag{26}$$

Using the coordinate transformation for the PMSM models in equation (18), the stator voltage equations of the PMSM can be deduced as

Table 1. Main mechanism and electromagnetism parameters of the AC servomotor-driven flexible manipulator.

Electromagnetism parameter	Value	Mechanism parameters	Value
Stator resistance (Ω)	5.60	Length of the flexible manipulator (m)	0.65
Rotor inertia (kg m^2)	0.38e−4	Density of the flexible manipulator (kg m^{-3})	7850.00
Stator self-inductance (H)	1.2e−2	Cross-sectional area of the flexible manipulator (m^2)	1.00e−4
Stator mutual inductance (H)	4.3e−4	Elastic modulus of the flexible manipulator (GPa)	197.00
Pole pairs	4	Screw lead (m)	5.00e−3
Flux linkage of the permanent magnet rotor (Wb)	0.13	Screw diameter (m)	3.00e−2
Rotation resistance coefficient of the motor rotor	0.001	Slider quality (kg)	1.56

$$\begin{cases} u_d = Ri_d + (L-H)\dfrac{\mathrm{d}}{\mathrm{d}t}i_d \\ \omega = \dot{\theta} \\ u_q = Ri_q + (L-H)\dfrac{\mathrm{d}}{\mathrm{d}t}i_q + \dfrac{\sqrt{6}}{2}\psi_f\omega \end{cases} \tag{27}$$

where u_d and u_q are the dq axis components of the stator voltage, ω is the speed of the PMSM, and i_d and i_q are the dq axis components of the stator current. Combining equations (24) to (27), equation (18) can be further decoupled as

$$\begin{cases} u_d = Ri_d + (L-M)\dfrac{\mathrm{d}}{\mathrm{d}t}i_d \\ u_q = Ri_q + (L-M)\dfrac{\mathrm{d}}{\mathrm{d}t}i_q + \dfrac{\sqrt{6}}{2}\psi_f\omega \\ \left(J + \dfrac{p}{2\pi}\rho AL\right)\ddot{\theta} + \sum_{k=1}^{4} m_k\ddot{q}_k(t) + R_n\omega \\ +\upsilon_c(W + M + \rho AL) = \dfrac{\sqrt{6}}{2}\psi_f i_q \\ \left\{\dfrac{p}{2\pi}m_k\ddot{\theta} + \rho A\ddot{q}_k(t) + \rho A\lambda_k^2 q_k(t) = 0\right\}_{k=1,2,3,4} \end{cases} \tag{28}$$

From the previous analysis, the partial decoupling model of the flexible manipulator of an AC servomotor-driven linear positioning platform is obtained. The quadrature axis current (i_q), which couples with the vibration modal coordinates of the flexible manipulator, can synthetically reflect the influence of the dynamic behavior of the PMSM on the electromechanical coupling vibration characteristics of the flexible manipulator.

Simulation examples

Because there are eight degrees of freedom in the global coupling dynamic models of the AC servomotor-driven flexible manipulator, of which mechanism and electromagnetism parameters are shown in Table 1, the numerical method is adopted to solve the models. In the simulation experiments, the tip vibrations of the flexible manipulator are analyzed.

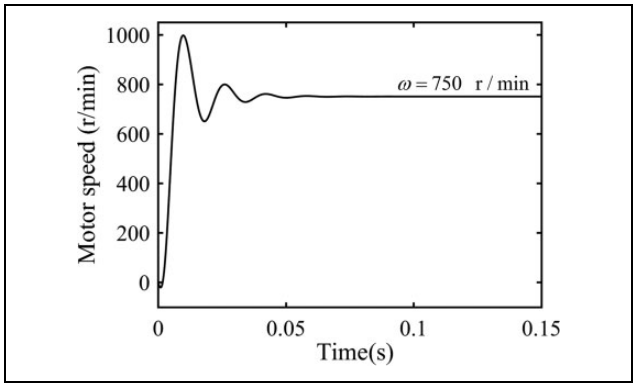

Figure 3. Speed of the PMSM ($f = 50$ Hz). AC: alternating current; PMSM: permanent magnet synchronous AC servomotor.

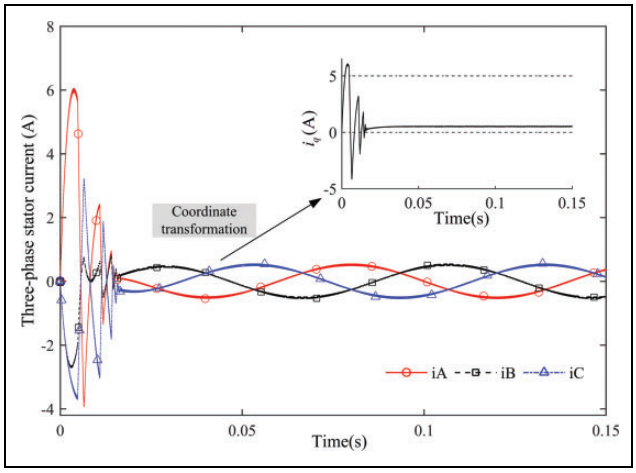

Figure 4. Current curve of the PMSM in the start-up phase. PMSM: permanent magnet synchronous AC servomotor.

According to the speed formula of synchronous motor ($\omega = 60f/p$), when the frequency of the input voltages is 50 Hz, the theoretical value of the output speed of the PMSM is 750 r min^{-1}. Then, the simulation value of the output speed, whichis also 750 r min^{-1}, is shown in Figure 3. Thus, the accuracy of the model is verified.

In the start-up phase, the three-phase stator current of the PMSM and the quadrature axis current, which is obtained by coordinate transforming from the three-phase stator current, are shown in Figure 4. It is found that the three-phase

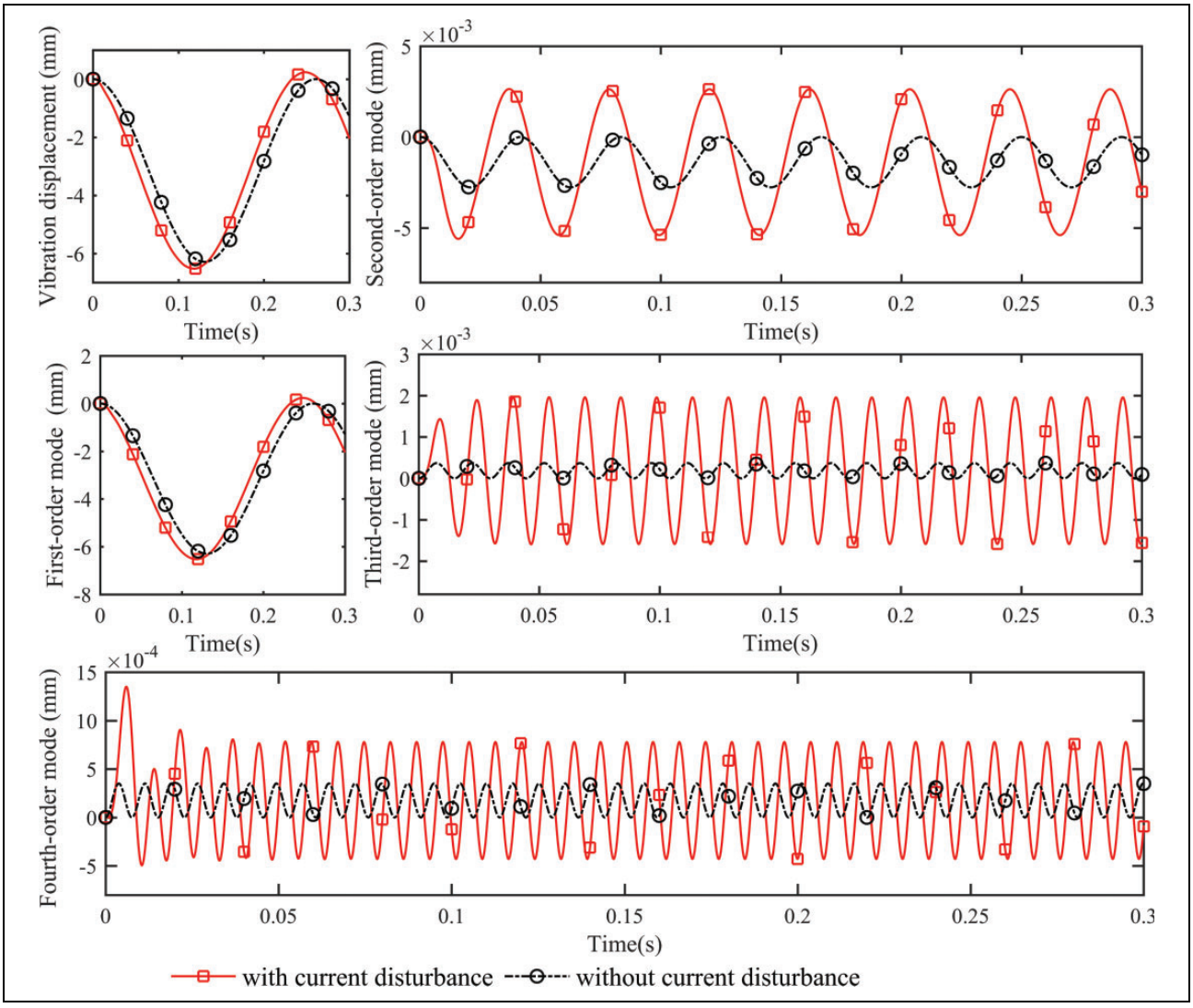

Figure 5. Response displacements of the first four order modes for the nonstationary start-up and ideal start-up of the PMSM. PMSM: permanent magnet synchronous AC servomotor.

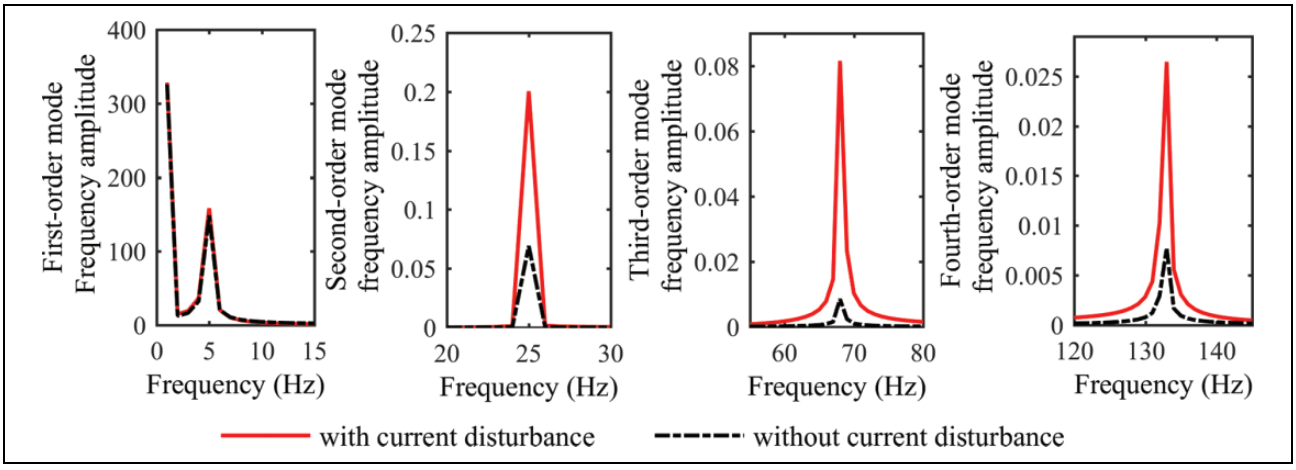

Figure 6. Frequency characteristics of the first four order modes for the nonstationary start-up and ideal start-up of the PMSM. PMSM: permanent magnet synchronous AC servomotor.

Table 2. Change rates of the response displacement for the first four order modes of the flexible manipulator.

	Response displacement (mm)		
	Ideal start-up	Nonstationary start-up	Change rates (%)
First-order mode	3.1448	3.3795	7.46
Second-order mode	0.0014	0.0041	192.86
Third-order mode	1.8462e−4	18.0000e−4	866.65
Fourth-order mode	1.7542e−4	6.0000e−4	241.88

stator current oscillates for some time before getting to steady state. Correspondingly, before the quadrature axis current reaches the steady values, there is also an oscillation process which is bound to affect the servo driving force of the linear positioning platform and subsequently influence the dynamic behavior of the flexible manipulator. Thus, it is very important to consider the effect of the start-up dynamic characteristics of the PMSM on the vibration characteristics of the flexible manipulator.

To the first four order modes of the flexible manipulator, the comparison of the response displacement and frequency characteristics for two states, the nonstationary start-up and ideal start-up of the PMSM, are shown in Figures 5 and 6. It can be seen that the current disturbances of the nonstationary start-up have great influence on the amplitude of the response displacement and almost have no effect on the response frequency. The results illustrated in Table 2—the change in rates of the response displacement for the first four order modes are 7.46%, 192.86%, 866.65%, and 241.88%, respectively—indicate that the influence of the current disturbances on the response displacement becomes obvious with the increase of the vibration modes. Furthermore, the effect on the response displacement of the third-order mode is the largest.

Further, in order to analyze the special influence mechanism of the current disturbances of the nonstationary start-up on the vibration characteristics of the flexible manipulator, under different target feed speed of the PMSM, the frequency characteristics of the current disturbance signals are presented in Figure 7. It can be seen that the feed speed of the PMSM has impacts on both the frequency component and its amplitude of the current disturbances. Furthermore, with the increase of the target speed, the dominant frequency component and its amplitude decrease and the reduction degree of the dominant frequency component is relatively slight. However, although the dominant frequency component of the current disturbances declines, it is always closer to the three-order natural frequency, which is 67.22 Hz, than other natural frequencies of the flexible manipulator. Finally, the results demonstrate that the current disturbances during the start-up process of the PMSM have the biggest impact on the response displacement of the three-order mode at which

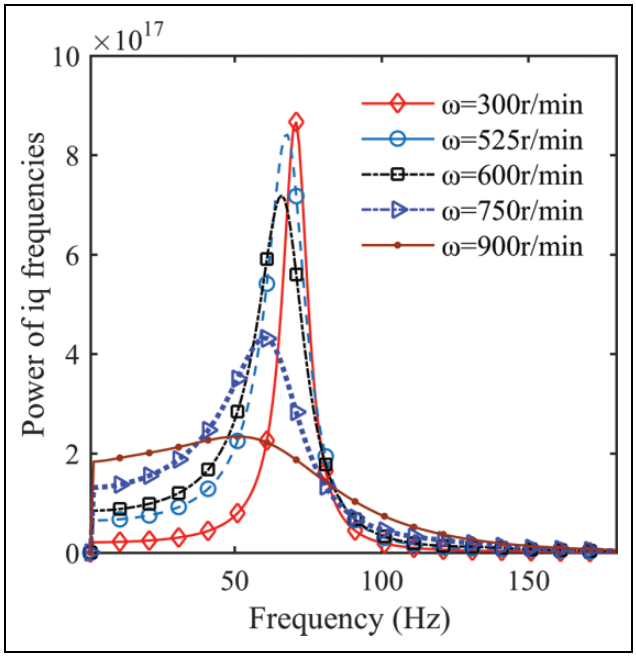

Figure 7. Power of q_i frequencies for different target feed speed.

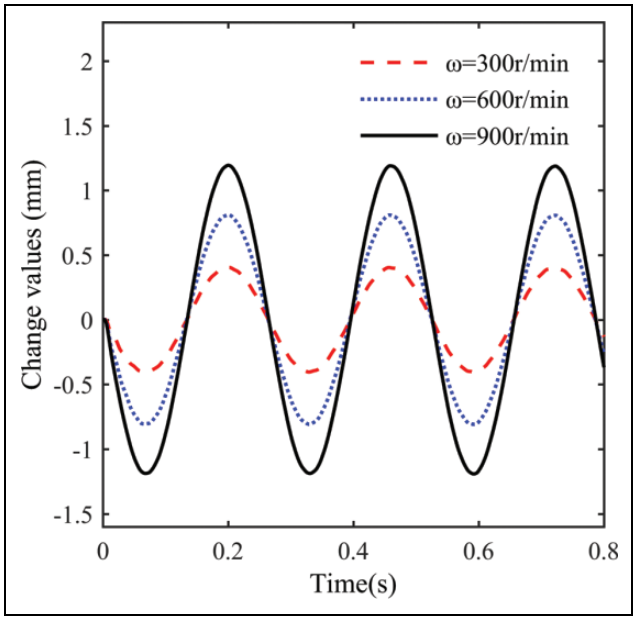

Figure 8. Influences of the current disturbances on the tip vibration for different target feed speed.

the resonance occurs. Unfortunately, the resonance of the response displacement of the three-order mode exists for long time, and it is of significant harm to the movement stability and high-precision positioning of the flexible manipulator.

Under the influences of the current disturbances, the change in values of the tip vibration displacement of the flexible manipulator for different target feed speed is shown in Figure 8. It can be obtained that the larger the

target speed, the more obvious changes of the tip vibration, which is manifested by the increase of the change in values of the tip vibration displacement.

Conclusions

Under the disturbance excitation of the motor stator current, the high-amplitude vibration and motion instability can be aroused in the flexible robot manipulator, especially in the motor start-up stage. Thus, this article presents the theoretical analysis and experimental simulation of the electromechanical coupling vibration characteristics for an AC servomotor-driven translational flexible manipulator. The global electromechanical coupling dynamic model of the flexible manipulator of an AC servomotor-driven linear positioning platform is constructed and the decoupling analysis of the model is completed. The results show that the influences of the current disturbances on the elastic vibration of the flexible manipulator become more obvious and the dominant frequency component of the current disturbances as well as its amplitude decreases, with the increase of the target speed. Moreover, the dominant frequency component of the current disturbances, of which reduction degree is relatively slight, is always close to the three-order natural frequency of the flexible manipulator. Then, the high-order mode vibration of the flexible manipulator is aroused. Above all, for the dynamic characteristics analysis and vibration control design of the flexible manipulator, the current disturbances of motor start-up should be considered more seriously. The analysis results are important guidance for the vibration control design and accurate positioning operations of the flexible robot manipulator in future work.

Author's Note

Author Yu-Fei Liu is currently affiliated to School of Mechanical and Automotive Engineering, Anhui Polytechnic University, Wuhu 241000, China.

Declaration of conflicting interests

The author(s) declared no potential conflicts of interest with respect to the research, authorship, and/or publication of this article.

Funding

The author(s) disclosed receipt of the following financial support for the research, authorship, and/or publication of this article: This research work was partially supported by the National Natural Science Foundation of China (No.51305444 and No.51307172), the Scientific and Technological Project of Jiangsu Province (BY2014028-06), the Six Talent Peaks Project in Jiangsu Province (ZBZZ-041), the Postgraduate Cultivation and Innovation Project of Jiangsu Province (KYZZ16-0213), and the Project Funded by the Priority Academic Program Development of Jiangsu Higher Education Institutions (PAPD).

References

1. Dupont PE, Lock J, Itkowitz B, et al. Design and control of concentric-tube robots. *IEEE Trans Robot* 2010; 26(2): 209–225.
2. Pereira E, Aphale SS, Feliu V, et al. Integral resonant control for vibration damping and precise tip-positioning of a single-link flexible manipulator. *IEEE/ASME Trans Mechatronics* 2011; 16(2): 232–240.
3. Mahvash M and Dupont PE. Stiffness control of surgical continuum manipulators. *IEEE Trans Robot* 2011; 27(2): 334–345.
4. Mohamed Z and Tokhi MO. Command shaping techniques for vibration control of a flexible robot manipulator. *Mechatronics* 2004; 14(1): 69–90.
5. Luo Q, Li D, and Zhou W. Studies on vibration isolation for a multiple flywheel system in variable configurations. *J Vibr Control* 2015; 21(1): 105–123.
6. Gouliaev VI and Zavrazhina TV. Dynamics of a flexible multi-link cosmic robot manipulator. *J Sound Vibr* 2001; 243(4): 641–657.
7. Nestinger SS, Chen B, and Cheng HH. A mobile agent-based framework for flexible automation systems. *IEEE/ASME Trans Mechatronics* 2010; 15(6): 942–951.
8. Moberg S, Wernholt E, Hanssen S, et al. Modeling and parameter estimation of robot manipulators using extended flexible joint models. *J Dyn Syst Meas Control* 2014; 136(3): 031005.
9. Gurses K, Buckham BJ, and Park EJ. Vibration control of a single-link flexible manipulator using an array of fiber optic curvature sensors and PZT actuators. *Mechatronics* 2009; 19(2): 167–177.
10. Ider SK and Korkmaz O. Trajectory tracking control of parallel robots in the presence of joint drive flexibility. *J Sound Vibr* 2009; 319(1): 77–90.
11. Dwivedy SK and Eberhard P. Dynamic analysis of flexible manipulators: a literature review. *Mech Mach Theory* 2006; 41(7): 749–777.
12. Coleman MP and McSweeney LA. Analysis and computation of the vibration spectrum of the Cartesian flexible manipulator. *J Sound Vibr* 2004; 274(1): 445–454.
13. Qiu ZC. Adaptive nonlinear vibration control of a Cartesian flexible manipulator driven by a ballscrew mechanism. *Mech Syst Signal Process* 2012; 30: 248–266.
14. Abe A. Trajectory planning for flexible Cartesian robot manipulator by using artificial neural network: numerical simulation and experimental verification. *Robotica* 2011; 29(05): 797–804.
15. Korayem MH, Bamdad M, Tourajizadeh H, et al. Experimental results for the flexible joint cable-suspended manipulator of ICaSbot. *Robotica* 2013; 31(06): 887–904.
16. Dadfarnia M, Jalili N, Xian B, et al. A Lyapunov-based piezoelectric controller for flexible Cartesian robot manipulators. *J Dyn Syst Meas Control* 2004; 126(2): 347–358.
17. Korayem MH, Nikoobin A, and Azimirad V. Trajectory optimization of flexible link manipulators in point-to-point motion. *Robotica* 2009; 27(06): 825–840.

18. Zhang X, Mills JK, and Cleghorn WL. Experimental implementation on vibration mode control of a moving 3-PRR flexible parallel manipulator with multiple PZT transducers. *J Vibr Control* 2010; 16(13): 2035–2054.
19. Pratiher B and Bhowmick S. Nonlinear dynamic analysis of a Cartesian manipulator carrying an end effector placed at an intermediate position. *Nonlin Dyn* 2012; 69(1–2): 539–553.
20. Pratiher B and Dwivedy SK. Non-linear dynamics of a flexible single link Cartesian manipulator. *Int J Non-lin Mech* 2007; 42(9): 1062–1073.
21. Dwivedy SK and Kar RC. Nonlinear response of a parametrically excited system using higher-order method of multiple scales. *Nonlin Dyn* 1999; 20(2): 115–130.
22. Liu YF, Li W, Yang XF, et al. Vibration response and power flow characteristics of a flexible manipulator with a moving base. *Shock Vibr* 2015; 2015: 1–8.
23. Li Z, Cai G, Huang Q, et al. Analysis of nonlinear vibration of a motor-linkage mechanism system with composite links. *J Sound Vibr* 2008; 311(3): 924–940.
24. Liou FW, Erdman AG, and Lin CS. Dynamic analysis of a motor-gear-mechanism system. *Mech Mach Theory* 1991; 26(3): 239–252.
25. Qiang L, Jianxin W, and Yan S. Dynamic optimization method on electromechanieal coupling system by exponential inertia weight particle swarm algorithm. *Chin J Mech Eng* 2009; 22(4): 602–607.